

HVD: HUMAN VISION-DRIVEN VIDEO REPRESENTATION LEARNING FOR TEXT-VIDEO RETRIEVAL

Zequn Xie^{1*}Xin Liu^{2*}

Boyun Zhang

Yuxiao Lin¹Sihang Cai¹Tao Jin^{1‡}¹ Zhejiang University² Southwestern University of Finance and Economics

ABSTRACT

The success of CLIP has driven substantial progress in text-video retrieval. However, current methods often suffer from “blind” feature interaction, where the model struggles to discern key visual information from background noise due to the sparsity of textual queries. To bridge this gap, we draw inspiration from human cognitive behavior and propose the **Human Vision-Driven (HVD)** model. Our framework establishes a coarse-to-fine alignment mechanism comprising two key components: the **Frame Features Selection Module (FFSM)** and the **Patch Features Compression Module (PFCM)**. FFSM mimics the human macro-perception ability by selecting key frames to eliminate temporal redundancy. Subsequently, PFCM simulates micro-perception by aggregating patch features into salient visual entities through an advanced attention mechanism, enabling precise entity-level matching. Extensive experiments on five benchmarks demonstrate that HVD not only captures human-like visual focus but also achieves state-of-the-art performance.

Index Terms— multi-modal representation learning, text-video retrieval, feature enhancement and interaction.

1. INTRODUCTION

With the rise of online video platforms and the increasing focus on integrated planning and multimodal intelligent agents [1, 2, 3, 4, 5, 6, 7, 8, 9, 10, 11], a large number of unlabeled videos are uploaded and downloaded. The emergence of text-video retrieval tasks has enabled these videos to be widely utilized and accessed. Recently, with the significant success of the large-scale text-image pretraining model CLIP [12] in representation learning, existing methods [13, 14] typically adopt CLIP to project text and video into a shared latent space, thereby establishing feature-level similarity relationships. To achieve more precise feature matching, current methods [15, 16, 17, 18] improve retrieval performance by leveraging granularity alignment and feature enhancement techniques. However, are these methods sufficient in terms of granularity alignment accuracy and feature enhancement effectiveness?

As illustrated in Fig. 1(a), given the text query “*a man is playing baseball*” and video frames, the frames show scenes of the man playing baseball as well as being interviewed. It is clear that only the first i frames (blue borders) are related to the text query, while the remaining frames (yellow borders) are unrelated. In the case of sparse queries, existing methods [19, 15, 20] typically incorporate all visual features into the interaction with text without considering feature effectiveness in Fig. 1(b). From the perspective of repeated human comparison, we focus more on the scenes related to “*baseball*” rather than the “*interview*.” Meanwhile, after identifying the

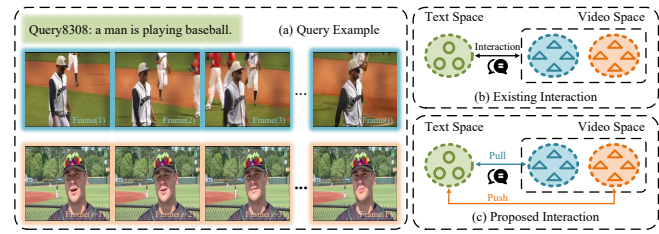


Fig. 1. Motivation. Not all visual features are relevant to the text query. Blue borders indicate the relevant frames, while yellow borders indicate the irrelevant frames.

key frames, it is necessary to repeatedly compare the keywords in the query with the visual entities in the frames, such as “*man*” or “*baseball*.” In other words, through this iterative comparison process, we can determine the optimal cross-modal feature interaction in Fig. 1(c). Therefore, we summarize this process into two stages: ① from a macro perspective, we observe all the frames of the video as a whole, selecting key frames that are highly relevant to the text query and thereby eliminating unrelated scenes; ② from a micro perspective, based on the key frames, we gradually extract key visual entities from the video frames, repeatedly comparing them with the keywords in the text query to refine feature interactions and ensure the accuracy of cross-modal feature alignment.

Existing methods [21, 22] have also conducted extensive explorations based on the above analysis. For example, UCoFiA [21] proposes a unified coarse-to-fine alignment model that effectively improves text-video retrieval performance from a comprehensive perspective. T-Mass [22] adopts a similarity-based feature modeling approach to expand text features, rather than directly aggregating frame features. In addition, feature enhancement methods [16, 23, 24] expand the receptive field. Although these methods achieve impressive retrieval performance, they fail to capture human interactive cognition and thus suffer from blind feature interaction. Specifically, ① Feature enhancement lacks robustness: when faced with distracting visual cues and sparse textual information, the enhanced features are affected by noise and lack stability. ② Feature interaction lacks precision: cross-modal feature matching and alignment are not accurate enough, resulting in blind spots or insufficient interaction of information.

To truly simulate human cognitive processes of alignment, we propose a novel text-video retrieval framework, named the **Human Vision-Driven (HVD)** model. Fig. 2 illustrates the overall framework. **First**, we propose a **Frame Features Selection Module (FFSM)** to accommodate the human macro-level alignment process. FFSM selects key video frames related to the text query based on similarity, effectively eliminating redundant and irrelevant frames

* Equal contribution.

† Corresponding author.

while retaining the patch features necessary for fine-grained alignment, thereby achieving a certain level of feature accuracy at the macro level. **Second**, we propose a **Patch Features Compression Module (PFCM)** to align with the human micro-level alignment process. The core of PFCM lies in compressing the patch features from the valid frames selected by FFSM, and then extracting the visual entity features that align with the textual word features. Specifically, we use the K-Nearest-Neighbor-based density peaks clustering algorithm, *i.e.*, DPC-KNN [25], to aggregate the patch features. Meanwhile, to emphasize important patches and capture the spatial relationships between patches, we introduce importance scores and attention weights to re-represent the patch features. Finally, through repeated aggregation and re-representation, we can obtain entity features at the word feature level. **Third**, the two modules work collaboratively to achieve video feature selection and compression, eliminating the need to consider complex text alignment strategies in subsequent stages. Experiments on five benchmarks demonstrate that HVD achieves state-of-the-art retrieval performance.

2. METHODS

2.1. Preliminaries

Let $\mathcal{D} = (\mathcal{T}, \mathcal{V})$ denote a language and vision dataset, where \mathcal{T} is a set of texts, and \mathcal{V} is a set of videos. The goal of text-video retrieval is to rank the relevance between a text query $t \in \mathcal{T}$ and video set \mathcal{V} . Recent works [13, 14, 22] have shown CLIP's strong performance in modality feature representation, inspiring us to employ CLIP as our backbone. Specifically, a video $v \in \mathcal{V}$ consists of N_f sequential frames $[f_1, f_2, \dots, f_{N_f}] \in \mathbb{R}^{N_f \times H \times W \times C}$, where each frame is divided into N_p patches $[p_1, p_2, \dots, p_{N_p}] \in \mathbb{R}^{N_p \times P \times P \times C}$ with $P \times P$ size. Following CLIP [12], we utilize the CLIP visual encoder to extract the patch features $V_p = [p_0, p_1, \dots, p_{N_p}] \in \mathbb{R}^{(N_p+1) \times D}$ of each frame, where p_0 represents the [CLS] token of the current frame. We aggregate the [CLS] tokens of all video frames to obtain the frame features $V_f = [f_1, f_2, \dots, f_{N_f}] \in \mathbb{R}^{N_f \times D}$. Similarly, given a text query $t \in \mathcal{T}$, we leverage the CLIP text encoder to extract word features $T_w = [w_{\text{BOS}}, w_1, w_2, \dots, w_{N_w}, w_{\text{EOS}}] \in \mathbb{R}^{(N_w+2) \times D}$, where N_w denotes the length of word sequences, and [BOS] and [EOS] tokens mark the beginning and end of a text sequence, respectively. We take the representation of the [EOS] token as the sentence feature $T_s = [s] \in \mathbb{R}^{1 \times D}$. The overall video and text features extraction process is illustrated in Fig. 2(1).

Feature interaction refers to the process of computing the similarity between textual and visual features, and mean pooling is the most direct method, *e.g.*, between T_s and V_f :

$$S_{T_s, V_f} = \frac{\mathbf{T}_s \cdot \mathbf{V}_f}{\|\mathbf{T}_s\| \cdot \|\mathbf{V}_f\|}, \quad (1)$$

where $\mathbf{V}_f = \frac{1}{N_f} \sum_i^{N_f} V_{f,i}$. Therefore, the sentence-frame cross-modal contrastive loss \mathcal{L}_{T_s, V_f} can be formulated as:

$$\begin{aligned} \mathcal{L}_{T_s, V_f} = & -\frac{1}{2} \left(\frac{1}{B} \sum_{i=1}^B \log \frac{\exp(S_{T_s^i, V_f^i}/\tau)}{\sum_{j=1}^B \exp(S_{T_s^i, V_f^j}/\tau)} \right. \\ & \left. + \frac{1}{B} \sum_{i=1}^B \log \frac{\exp(S_{T_s^i, V_f^i}/\tau)}{\sum_{j=1}^B \exp(S_{T_s^j, V_f^i}/\tau)} \right), \end{aligned} \quad (2)$$

where B is the batch size, τ is the temperature hyper-parameter, and $S_{T_s^i, V_f^j}$ represents the similarity between the i^{th} text sentence

feature and the j^{th} video frame feature in the entire batch. This loss function maximizes the similarity of positive pairs and minimizes the similarity of negative pairs. Similarly, \mathcal{L}_{T_w, V_f} , \mathcal{L}_{T_s, V_p} , and \mathcal{L}_{T_s, V_f} can be computed.

2.2. Frame Features Selection Module

In this part, we propose a **Frame Features Selection Module (FFSM)** from a human macro alignment perspective, as shown in Fig. 2(2). First, when aligning text and video, we, as humans, first read the overall sentence feature $T_s = [s] \in \mathbb{R}^{1 \times D}$, and then compare it with each video frame features $V_f = [f_1, f_2, \dots, f_{N_f}] \in \mathbb{R}^{N_f \times D}$ to identify the effective frames $V_f^* \in \mathbb{R}^{N_f^* \times D}$, where $N_f^* < N_f$. Next, from a human-centric perspective, the selection of effective frames V_f^* can be directly based on the similarity $S_{T_s, V_f} = \frac{s \cdot f}{\|s\| \cdot \|f\|} \in \mathbb{R}^{1 \times N_f}$ between T_s and V_f . Finally, we select the top- N_f^* frames V_f^* from V_f based on S_{T_s, V_f} :

$$V_f^* = \{f_i\}, i \in \arg \max_i S_{T_s, V_f}, i = 1, 2, \dots, N_f^*. \quad (3)$$

In addition, the patch features are also updated from V_p to V_p^* .

2.3. Patch Features Compression Module

In this part, we propose a **Patch Features Compression Module (PFCM)** from a human micro alignment perspective, as shown in Fig. 2(3). First, we focus on the patch features $V_p^* = N_f^* \times [p_1, p_2, \dots, p_{N_p}] \in \mathbb{R}^{N_f^* \times N_p \times D}$ under the FFSM. This step, benefiting from global features selection, not only focuses on key frames but also significantly reduces the number of patch features. Next, we further compress the patch features V_p^* from a human cognitive perspective.

Specifically, we utilize a variant of the k -nearest neighbor-based density peaks clustering algorithm (DPC-KNN) [25]. Given patch features V_p^* , we compute the local density ρ_i of each patch p_i according to its k -nearest neighbors: $\rho_i = \exp(-\frac{1}{k} \sum ||p_i - p_j||_2)$, where $p_j \in \text{KNN}(p_i)$, and $\text{KNN}(p_i)$ denotes the k -nearest neighbors of the patch p_i . Then, we compute the distance indicator δ_i of each patch:

$$\delta_i = \begin{cases} \min ||p_i - p_j||_2, & \rho_i < \rho_j, \\ \max ||p_i - p_j||_2, & \rho_i \geq \rho_j. \end{cases} \quad (4)$$

Intuitively, the patch p_i with a larger local density ρ_i and distance indicator δ_i is more likely to become a cluster center. We determine a cluster center by selecting the patches with the highest scores $\rho_i \times \delta_i$, and then merge the neighboring patches. The merged patch p_i^* is fed into a transformer block as query Q , and the original patch p_i is used as key K and value V is added to the attention weight as follows:

$$\text{Attention}(Q, K, V) = \text{softmax} \left(\frac{QK^T}{\sqrt{D}} \right) V, \quad (5)$$

By introducing the clustering algorithm and the attention mechanism, PFCM not only reduces the number of patch features but also focuses on key features and spatial relationships. Finally, we iteratively apply PFCM to compress and aggregate patch features, reducing their number.

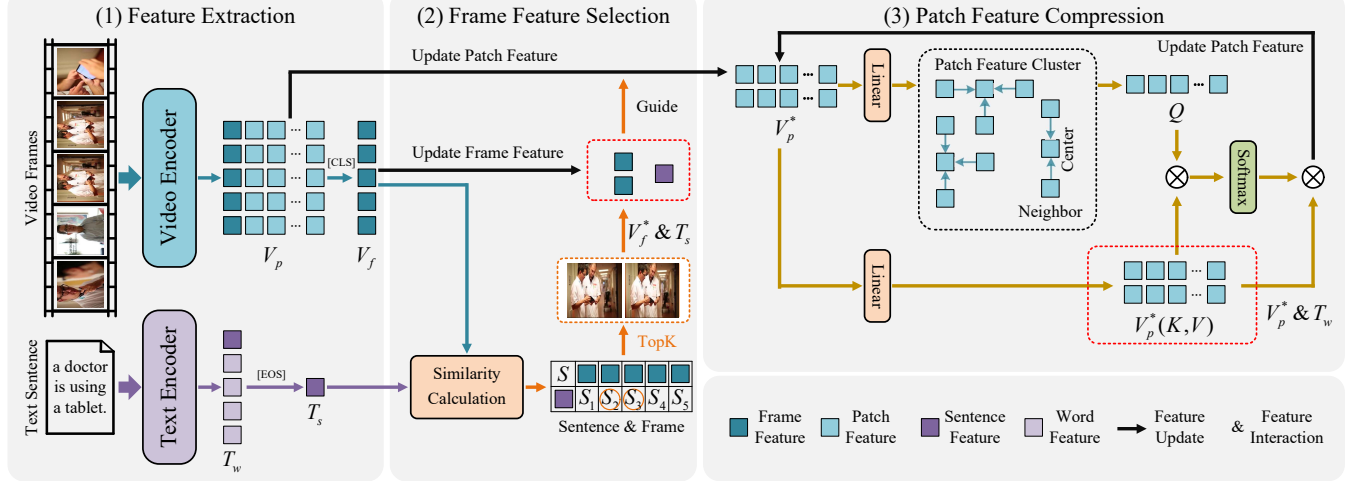


Fig. 2. Framework. (1) CLIP Feature Extraction Module. (2) Frame Feature Selection Module: selects keyframes that best match the text from a human global perspective based on text-frame similarity. (3) Patch Feature Compression Module: compresses visual features from a human local perspective, focusing on the most informative patch regions.

2.4. Training and Sampling

To effectively integrate global and local visual information, we combine the macro-level frame features V_f^* derived from FFSM and the micro-level patch features V_p^* obtained from PFCM. Based on these representations, we compute the corresponding similarity scores: the sentence-frame similarity S_{T_s, V_f^*} and the word-entity similarity S_{T_w, V_p^*} . The overall training objective is to jointly minimize the losses from both perspectives. Thus, we compute the total loss \mathcal{L}_{total} as defined in Eq. 6:

$$\mathcal{L}_{total} = \mathcal{L}_{T_s, V_f^*} + \mathcal{L}_{T_w, V_p^*}. \quad (6)$$

During the inference phase, we calculate the final similarity between the text query and the video by aggregating both the global similarity S_{T_s, V_f^*} and the local similarity S_{T_w, V_p^*} to determine the retrieval ranking.

3. EXPERIMENTS

3.1. Experimental Settings

We evaluate HVD on five benchmarks: MSRVTT, DiDeMo, LSMDC, ActivityNet, and Charades. Performance is reported using R@K (K=1, 5, 10), MdR, and MnR. Utilizing CLIP [12] as the backbone, we train the model for 5 epochs with a batch size of 32 and a feature dimension of 512. The input is configured with $N_f = 12$ sampled frames and a maximum text length of $N_w = 24$. Both frame and patch retention ratios are set to 0.5. Additional implementation details follow standard protocols [13, 14, 15, 22, 24].

3.2. Experimental Performance

In Tab. 1, we report the retrieval performance of HVD on the MSRVTT dataset, achieving an R@1 of 48.8. Compared with HBI [15], this represents an improvement of 0.2, indicating that our method benefits from visual feature selection and compression. In Tab. 2, we further evaluate the retrieval performance of HVD on datasets such as DiDeMo. HVD achieves consistent performance

improvements on both the long-video DiDeMo and the short-text LSMDC.

Methods	MSRVTT (Text→Video)				
	R@1↑	R@5↑	R@10↑	MdR↓	MnR↓
Clip4clip [13]	44.5	71.4	81.6	2.0	15.3
X-Pool [14]	46.9	72.8	82.2	2.0	14.3
UATVR [16]	47.5	73.9	83.5	2.0	12.3
HBI [15]	48.6	74.6	83.4	2.0	12.0
EERCF [24]	47.8	74.1	84.1	2.0	-
BiHSSP [26]	48.1	74.0	84.1	2.0	12.1
HVD (Ours)	48.8	75.2	85.3	2.0	11.7

Table 1. Retrieval performance on the MSRVTT datasets. “↑” means that higher is better. “↓” means that lower is better.

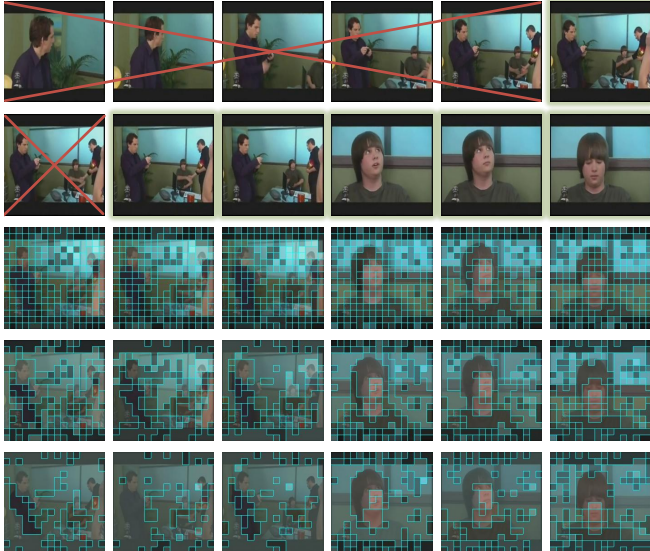
Methods	DiDeMo		LSMDC	
	R@1↑	R@10↑	R@1↑	R@10↑
EMCL-Net [27]	45.3	82.3	23.9	53.7
X-Pool [14]	44.6	82.0	25.2	53.5
CLIP-VIP [28]	48.6	84.4	25.6	54.4
DiCoSA [19]	45.7	83.5	25.4	54.0
HVD (Ours)	48.9	84.0	26.1	57.0

Methods	ActivityNet		Charades	
	R@1↑	R@10↑	R@1↑	R@10↑
Clip4clip [13]	40.5	83.6	9.9	36.8
HBI [15]	42.2	84.6	-	-
T-Mass [22]	-	-	14.2	48.3
HVD (Ours)	44.6	85.7	18.8	54.6

Table 2. Retrieval performance on other datasets.

In Tab. 3, we perform an ablation study on HVD’s FFSM and PFCM, and using \mathcal{L}_{T_s, V_f} as the baseline in Eq. 1 (R1). The experiments show that combining macro frame selection (R2) with micro patch compression (R3) achieves the best retrieval performance

Query1404: there is a t-shirt boy is talking with someone.



Query1527: pekids using a mobile watch.

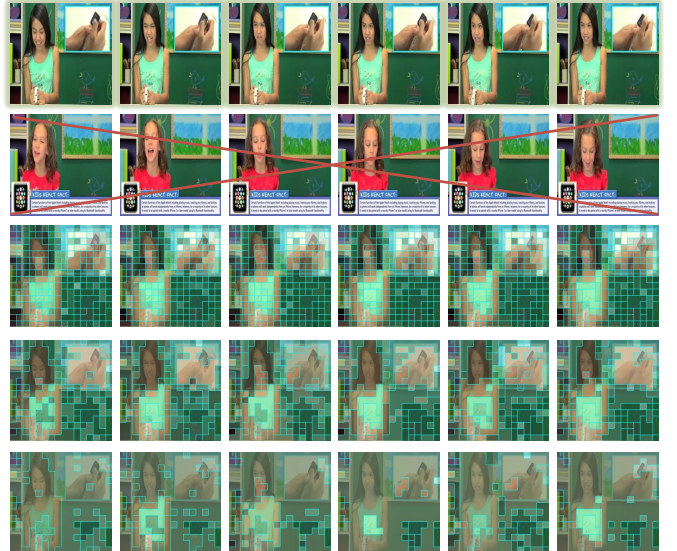


Fig. 3. Visualization. Red lines indicate the frame features that are selected for removal.

(R4). This further indicates a close relationship between FFSM and PFCM: the former provides refined information to the latter, while the latter complements the former with additional details.

Rx	FFSM	PFCM	R@1↑	R@5↑	R@10↑	MnR↓
R1			44.6	71.0	81.7	15.3
R2	✓		44.7	72.5	82.4	14.6
R3		✓	46.3	74.8	83.7	12.2
R4	✓	✓	48.8	75.2	85.3	11.7

Table 3. Ablation studies of FFSM and PFCM.

(\hbar, λ)	$N_f^* = \hbar N_f, N_p^* = \lambda N_p$				MSRVTT	
	N_f^*	N_p^*	N_p^*	N_p^*	R@1↑	R@10↑
(1.00, 1.00)	12	600	600	600	44.6	81.7
(0.25, 0.50)	3	90	45	23	44.2	81.5
(0.50, 0.75)	6	225	169	127	46.2	84.7
(0.50, 0.50)	6	150	75	38	48.8	85.3
(0.50, 0.25)	6	75	19	5	47.1	84.2
(0.75, 0.50)	9	225	113	56	48.3	84.7

Table 4. Ablation studies of factor \hbar and factor λ .

To further investigate the impact of feature selection and compression levels on retrieval performance, we set them to \hbar and λ , respectively, as shown in Tab. 4. \hbar and λ denote the proportions of retained video frames and image patches, respectively. When setting $(\hbar, \lambda) = (0.50, 0.50)$, HVD achieves the best retrieval performance, further indicating that selecting an appropriate granularity can enhance feature interactions. Based on this parameter setting, we visualize the process of video frame selection and patch feature compression during training in Fig. 3. The non-red regions indicate frames used for text interaction. The last three rows show the results of three

consecutive PFCM operations, with the number of features involved in the interaction gradually decreasing.

4. CONCLUSION

In this paper, we propose HVD, a human-vision-driven video representation model that integrates frame selection (FFSM) and patch compression (PFCM) to improve text–video retrieval performance. Guided by human macroscopic and microscopic perspectives, these modules jointly improve video representations at frame and patch levels, addressing both coarse- and fine-grained alignment. We evaluate HVD on five benchmark datasets, including MSRVTT, DiDeMo, LSMDC, ActivityNet, and Charades, achieving state-of-the-art retrieval performance. In addition, we further validate the effectiveness and intuitiveness of the proposed modules through ablation studies on FFSM, PFCM, and hyper-parameter settings, as well as visualizations. We hope that this work will provide inspiration to the video retrieval community.

5. REFERENCES

- [1] Runhao Liu, Ziming Chen, You Li, Zequn Xie, and Peng Zhang, “Integrated planning and machine-level scheduling for high-mix discrete manufacturing: A profit-driven heuristic framework,” 2025.
- [2] Q. He, “A unified metric architecture for ai infrastructure: A cross-layer taxonomy integrating performance, efficiency, and cost,” *arXiv preprint arXiv:2511.21772*, 2025.
- [3] Zhaolu Kang, Junhao Gong, Qingxi Chen, Hao Zhang, Jiaxin Liu, Rong Fu, Zhiyuan Feng, Yuan Wang, Simon Fong, and Kaiyue Zhou, “Multimodal multi-agent empowered legal judgment prediction,” 2026.
- [4] Weihai Lu, Yu Tong, and Zhiqiu Ye, “Dammfnd: Domain-aware multimodal multi-view fake news detection,” in *Proceedings of the AAAI Conference on Artificial Intelligence*, 2025, vol. 39, pp. 559–567.

[5] Yu Tong, Weihai Lu, Xiaoxi Cui, Yifan Mao, and Zhejun Zhao, “Dapt: Domain-aware prompt-tuning for multimodal fake news detection,” in *Proceedings of the 33rd ACM International Conference on Multimedia*, 2025, pp. 7902–7911.

[6] Dingyuan Liu, Qiannan Shen, and Jiaci Liu, “The health-wealth gradient in labor markets: Integrating health, insurance, and social metrics to predict employment density,” *Computation*, vol. 14, no. 1, pp. 22, 2026.

[7] Wenxi Sun, Qiannan Shen, Yijun Gao, Qinkai Mao, Tongsong Qi, and Shuo Xu, “Objective over architecture: Fraud detection under extreme imbalance in bank account opening,” *Computation*, vol. 13, no. 12, pp. 290, 2025.

[8] Shuang Zeng, Xinyuan Chang, Mengwei Xie, Xinran Liu, Yifan Bai, Zheng Pan, Mu Xu, and Xing Wei, “Futuresightdrive: Thinking visually with spatio-temporal cot for autonomous driving,” *arXiv preprint arXiv:2505.17685*, 2025.

[9] Shilin Lu, Zilan Wang, Leyang Li, Yanzhu Liu, and Adams Wai-Kin Kong, “Mace: Mass concept erasure in diffusion models,” in *Proceedings of the IEEE/CVF Conference on Computer Vision and Pattern Recognition*, 2024, pp. 6430–6440.

[10] Shilin Lu, Yanzhu Liu, and Adams Wai-Kin Kong, “Tf-icon: Diffusion-based training-free cross-domain image composition,” in *Proceedings of the IEEE/CVF International Conference on Computer Vision*, 2023, pp. 2294–2305.

[11] Shilin Lu, Zihan Zhou, Jiayou Lu, Yuanzhi Zhu, and Adams Wai-Kin Kong, “Robust watermarking using generative priors against image editing: From benchmarking to advances,” *arXiv preprint arXiv:2410.18775*, 2024.

[12] Alec Radford, Jong Wook Kim, Chris Hallacy, Aditya Ramesh, Gabriel Goh, Sandhini Agarwal, Girish Sastry, Amanda Askell, Pamela Mishkin, Jack Clark, et al., “Learning transferable visual models from natural language supervision,” in *International conference on machine learning*. PMLR, 2021, pp. 8748–8763.

[13] Huashao Luo, Lei Ji, Ming Zhong, Yang Chen, Wen Lei, Nan Duan, and Tianrui Li, “Clip4clip: An empirical study of clip for end to end video clip retrieval and captioning,” *Neurocomputing*, vol. 508, pp. 293–304, 2022.

[14] Satya Krishna Gorti, Noël Voutsis, Junwei Ma, Keyvan Golestan, Maksims Volkovs, Animesh Garg, and Guangwei Yu, “X-pool: Cross-modal language-video attention for text-video retrieval,” in *Proceedings of the IEEE/CVF conference on computer vision and pattern recognition*, 2022, pp. 5006–5015.

[15] Peng Jin, Jinfa Huang, Pengfei Xiong, Shangxuan Tian, Chang Liu, Xiangyang Ji, Li Yuan, and Jie Chen, “Video-text as game players: Hierarchical banzhaf interaction for cross-modal representation learning,” in *Proceedings of the IEEE/CVF Conference on Computer Vision and Pattern Recognition*, 2023, pp. 2472–2482.

[16] Bo Fang, Wenhao Wu, Chang Liu, Yu Zhou, Yuxin Song, Weiping Wang, Xiangbo Shu, Xiangyang Ji, and Jingdong Wang, “Uatvr: Uncertainty-adaptive text-video retrieval,” in *Proceedings of the IEEE/CVF International Conference on Computer Vision*, 2023, pp. 13723–13733.

[17] Zequn Xie, Boyun Zhang, Yuxiao Lin, and Tao Jin, “Delving deeper: Hierarchical visual perception for robust video-text retrieval,” 2026.

[18] Fan Zhang, Gongguan Chen, Hua Wang, and Caiming Zhang, “Cf-dan: Facial-expression recognition based on cross-fusion dual-attention network,” *Computational Visual Media*, vol. 10, no. 3, pp. 593–608, 2024.

[19] Peng Jin, Hao Li, Zesen Cheng, Jinfa Huang, Zhennan Wang, Li Yuan, Chang Liu, and Jie Chen, “Text-video retrieval with disentangled conceptualization and set-to-set alignment,” in *Proceedings of the Thirty-Second International Joint Conference on Artificial Intelligence, IJCAI-23*, 2023, pp. 938–946, International Joint Conferences on Artificial Intelligence Organization.

[20] Zequn Xie, Chuxin Wang, Yeqiang Wang, Sihang Cai, Shulei Wang, and Tao Jin, “Chat-driven text generation and interaction for person retrieval,” in *Proceedings of the 2025 Conference on Empirical Methods in Natural Language Processing*, 2025, pp. 5259–5270.

[21] Ziyang Wang, Yi-Lin Sung, Feng Cheng, Gedas Bertasius, and Mohit Bansal, “Unified coarse-to-fine alignment for video-text retrieval,” in *Proceedings of the IEEE/CVF International Conference on Computer Vision*, 2023, pp. 2816–2827.

[22] Jiamian Wang, Guohao Sun, Pichao Wang, Dongfang Liu, Sohail Dianat, Majid Rabbani, Raghavveer Rao, and Zhiqiang Tao, “Text is mass: Modeling as stochastic embedding for text-video retrieval,” in *Proceedings of the IEEE/CVF Conference on Computer Vision and Pattern Recognition*, 2024, pp. 16551–16560.

[23] Xiaojie Jin, Bowen Zhang, Weibo Gong, Kai Xu, Xueqing Deng, Peng Wang, Zhao Zhang, Xiaohui Shen, and Jiashi Feng, “Mv-adapter: Multimodal video transfer learning for video text retrieval,” in *Proceedings of the IEEE/CVF Conference on Computer Vision and Pattern Recognition*, 2024, pp. 27144–27153.

[24] Kaibin Tian, Yanhua Cheng, Yi Liu, Xinglin Hou, Quan Chen, and Han Li, “Towards efficient and effective text-to-video retrieval with coarse-to-fine visual representation learning,” in *Proceedings of the AAAI Conference on Artificial Intelligence*, 2024, vol. 38, pp. 5207–5214.

[25] Mingjing Du, Shifei Ding, and Hongjie Jia, “Study on density peaks clustering based on k-nearest neighbors and principal component analysis,” *Knowledge-Based Systems*, vol. 99, pp. 135–145, 2016.

[26] Yang Liu, Shudong Huang, Deng Xiong, and Jiancheng Lv, “Learning dynamic similarity by bidirectional hierarchical sliding semantic probe for efficient text video retrieval,” in *Proceedings of the AAAI Conference on Artificial Intelligence*, 2025, vol. 39, pp. 5667–5675.

[27] Peng Jin, Jinfa Huang, Fenglin Liu, Xian Wu, Shen Ge, Guoli Song, David Clifton, and Jie Chen, “Expectation-maximization contrastive learning for compact video-and-language representations,” *Advances in neural information processing systems*, vol. 35, pp. 30291–30306, 2022.

[28] Hongwei Xue, Yuchong Sun, Bei Liu, Jianlong Fu, Ruihua Song, Houqiang Li, and Jiebo Luo, “Clip-vip: Adapting pre-trained image-text model to video-language alignment,” in *The Eleventh International Conference on Learning Representations*, 2022.